AGU PUBLICATIONS

Geophysical Research Letters

RESEARCH LETTER
10.1002/2016GL070916

Key Points:
- Identification of new sulfur oxides in the Venusian atmosphere
- Near-UV absorption of OSSO matches missing absorber on Venus
- Important sulfur oxide reservoir found below 70 km altitude

Supporting Information:
- Supporting Information S1
- Table S1
- Table S2

Correspondence to:
H. G. Kjaergaard,
hgk@chem.ku.dk

Citation:
Frandsen, B. N., P. O. Wennberg, and H. G. Kjaergaard (2016), Identification of OSSO as a near-UV absorber in the Venusian atmosphere, *Geophys. Res. Lett.*, *43*, 11,146–11,155, doi:10.1002/2016GL070916.

Received 30 MAR 2016
Accepted 21 SEP 2016
Published online 3 NOV 2016

Identification of OSSO as a near-UV absorber in the Venusian atmosphere

Benjamin N. Frandsen[1], Paul O. Wennberg[2], and Henrik G. Kjaergaard[1]

[1]Department of Chemistry, University of Copenhagen, Copenhagen, Denmark, [2]Division of Engineering and Applied Science and Division of Geological and Planetary Sciences, California Institute of Technology, Pasadena, California, USA

Abstract The planet Venus exhibits atmospheric absorption in the 320–400 nm wavelength range produced by unknown chemistry. We investigate electronic transitions in molecules that may exist in the atmosphere of Venus. We identify two different S_2O_2 isomers, *cis*-OSSO and *trans*-OSSO, which are formed in significant amounts and are removed predominantly by near-UV photolysis. We estimate the rate of photolysis of *cis*- and *trans*-OSSO in the Venusian atmosphere and find that they are good candidates to explain the enigmatic 320–400 nm near-UV absorption. Between 58 and 70 km, the calculated OSSO concentrations are similar to those of sulfur monoxide (SO), generally thought to be the second most abundant sulfur oxide on Venus.

1. Introduction

In 1974, the first spacecraft passed by Venus and took high-resolution spectra of the planet [*Dunne*, 1974; *Murray et al.*, 1974]. Since then, several additional spacecraft have visited the planet; the Venus Express from the European Space Agency was the most recent mission [*Titov et al.*, 2006]. Ground-based studies of Venus have also taken place [*Barker*, 1979; *Sandor et al.*, 2010; *Travis*, 1975, and references therein]. Many features of the Venusian atmosphere have been studied, such as the atmospheric distribution of SO and SO_2 and the interannual variation in their concentration, the sulfuric acid cycle, and carbonyl sulfide (OCS) chemistry [*Esposito et al.*, 1979; *Seiff et al.*, 1985; *Belyaev et al.*, 2012; *Sandor et al.*, 2010; *Esposito*, 1984; *Esposito et al.*, 1988; *Marcq et al.*, 2011; *Encrenaz et al.*, 2012; *Marcq et al.*, 2013; *Encrenaz et al.*, 2013; *Jessup et al.*, 2015; *Zhang et al.*, 2010; *Palmer and Williams*, 1975; *Yung et al.*, 2009; *Krasnopolsky*, 2008; *Arney et al.*, 2014; *Marcq et al.*, 2008, 2006, 2005]. Extensive modeling of the atmospheric chemistry on Venus has also been done [*Krasnopolsky*, 2012; *Zhang et al.*, 2012].

One of the characteristic features of the Venusian atmosphere is the strong absorption observed between 320 to 400 nm [*Ross*, 1928; *Coffeen*, 1971; *Barker*, 1979; *Pollack et al.*, 1980]. This absorption is heterogeneous with some regions showing roughly 20% higher absorption than others [*Molaverdikhani et al.*, 2012]. Many possible molecular absorbers have been suggested, but so far none have been demonstrated to fit satisfactorily the observations [*Krasnopolsky*, 2006; *Molaverdikhani et al.*, 2012; *Pollack et al.*, 1979; *Barker et al.*, 1975; *Travis*, 1975; *Pollack et al.*, 1980; *Zasova et al.*, 1981; *Markiewicz et al.*, 2014; *Toon et al.*, 1982; *Hartley et al.*, 1989; *Na and Esposito*, 1997]. The inhomogeneous distribution (and therefore short lifetime) of the unknown absorber suggests gaseous molecules, while the rich-sulfur chemistry on Venus makes sulfur-containing absorbers likely candidates [*Molaverdikhani et al.*, 2012; *Na and Esposito*, 1997; *Zhang et al.*, 2012; *Parkinson et al.*, 2015; *Esposito et al.*, 1988]. Furthermore, the unknown absorber is correlated with SO_2 [*Marcq et al.*, 2013; *Titov et al.*, 2008; *Esposito and Travis*, 1982]. The near-UV absorption occurs within the top cloud layer (beginning at ~60 km altitude) and in the mesosphere (beginning at 67±2 km altitude) [*Lee et al.*, 2015; *Molaverdikhani et al.*, 2012; *Rossow et al.*, 1990; *Haus et al.*, 2015, 2016]. The sulfur oxides, SO and SO_2, are abundant in the Venusian atmosphere with mixing ratios of approximately 7 to 30 ppb for SO and 30 to 500 ppb for SO_2 at 64 km altitude near the equator [*Na et al.*, 1994, 1990; *Belyaev et al.*, 2012; *Sandor et al.*, 2010]. The high concentration of SO means that SO dimers, S_2O_2, should also be present in the Venusian atmosphere. Based on computational studies, several different S_2O_2 isomers have been suggested to exist [*Marsden and Smith*, 1990; *Chen et al.*, 2004; *Goodarzi et al.*, 2010; *Murakami et al.*, 2003; *Ramírez-Solís et al.*, 2011].

Previously, the lowest energy S_2O_2 isomer, trigonal S_2O_2 (see Figure 1), was considered as being formed on Venus [*Krasnopolsky*, 2012]. This suggestion was based on a theoretical study [*Marsden and Smith*, 1990].

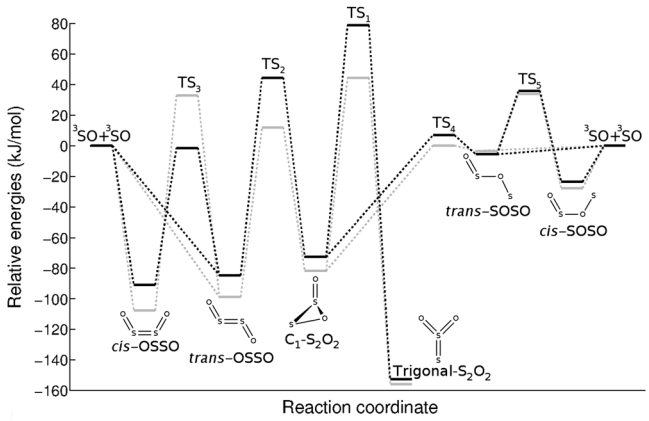

Figure 1. Overview of the stable singlet S_2O_2 isomers and the transition states (TS) connecting them. The relative energies are given as the ZPVE-corrected electronic energies using either CCSD(T)/cc-pV(T+d)Z (gray) or MRCI/cc-pV(T+d)Z on a [2,2]-CASSCF reference wave function (black).

However, in the microwave study by *Lovas et al.* [1974] a planar *cis*-OSSO isomer was identified as the only observed S_2O_2 isomer formed by recombination of SO molecules. An estimate of the rate constant for the SO+SO+M → $(SO)_2$+M reaction has been determined by *Herron and Huie* [1980]. They make no clear assignment of which $(SO)_2$ isomer was formed, however. Using quantum chemical calculations, we argue here that *cis*- and *trans*-OSSO are the products of this reaction and show that they both should be abundant and create significant opacity in the near-UV. Additional molecular species were investigated and rejected as significant near-UV absorbers on Venus. We discuss these species in the supporting information section S3 [*Vandaele et al.*, 1996].

2. Computational Methods

Minima and transition state geometries were optimized using the coupled-cluster singles, doubles and perturbative triples [CCSD(T)] method, and the multireference configuration interaction (MRCI) method with the cc-pV(T+d)Z basis set and default settings [*Raghavachari et al.*, 1989; *Dunning et al.*, 2001; *Lee and Taylor*, 1989; *Miliordos and Xantheas*, 2014]. We employed [2,2]-CAS reference wave functions for the MRCI calculations [*Sherrill and Schaefer*, 1999]. For all stationary points, a harmonic frequency calculation showed that the calculated minima had no imaginary vibrational frequencies and that the transitions states had exactly one imaginary frequency. The frequency calculation was also used to provide the zero-point vibrational energy (ZPVE) correction to electronic energies. Both CCSD(T) and MRCI perform well compared to full configuration interaction (CI) [*Werner and Knowles*, 1988; *Rossi et al.*, 1999] and are both known to provide results of near experimental accuracy results [*Jurečka et al.*, 2006; *Shamasundar et al.*, 2011].

The potential energy surface of $^3SO+^3SO$, reacting to form the singlet of *cis*-OSSO, *trans*-OSSO, *cis*-SOSO, and *trans*-SOSO, respectively, was calculated with unrestricted density functional theory (DFT) (see supporting information Figure S3) [*Becke*, 1993; *Lee et al.*, 1988]. Further potential energy surface calculations were done using resolution of identity spin component scaled Møller-Plesset second-order perturbation theory (RI-SCS-MP2) method with the cc-pVDZ basis set [*Feyereisen et al.*, 1993; *Bernholdt and Harrison*, 1996; *Grimme*, 2003].

The geometry of the second excited state of *cis*- and *trans*-OSSO was optimized using the MRCI/aug-cc-pV(T+d)Z method based on a [8,6]-CASSCF reference, to find if the excited state is dissociative or not. This complete active space was chosen to include all electronic configurations contributing with a CI vector larger than 0.05 in the excited state, which was found by analyzing the CI vectors from a [12,12]-CASSCF/aug-cc-pV(T+d)Z geometry optimization on the excited states.

Vertical excitation energies (Vee) and oscillator strengths (*f*) were calculated for the S_2O_2 isomers using the linear response coupled-cluster (LR-CC) methods: Iterative approximate coupled-cluster singles and doubles (CC2); full coupled-cluster singles and doubles (CCSD) with the basis sets aug-cc-pV(X+d)Z (X=D,T or Q); and the iterative approximate coupled-cluster singles, and doubles and triples (CC3) method with the basis sets

aug-cc-pV(X+d)Z for (X=D or T) [*Christiansen et al.*, 1995; *Purvis and Bartlett*, 1982; *Koch et al.*, 1997]. All linear response calculations on the S_2O_2 isomers and S_2O were carried out using the MRCI/cc-pV(T+d)Z optimized geometries. The convergence of the calculated electronic transition energies for *cis*- and *trans*-OSSO suggests that the uncertainty on the CC3 computed values is insignificant (less than ±2 nm for the 320–400 nm region), and the computed oscillator strength (integrated absorption cross section) has an accuracy of within ±20% (see supporting information Tables S13 and S14, and references *Lane and Kjaergaard* [2008] and *Kánnar and Szalay* [2014]).

DFT and TD-DFT calculations [*Becke*, 1993; *Lee et al.*, 1988; *Zhao and Truhlar*, 2008; *Chai and Head-Gordon*, 2008] were done with the Gaussian 09 quantum chemistry package [*Frisch et al.*, 2009]. CCSD(T), CASSCF, and MRCI calculations were done with the Molpro quantum chemistry package [*Werner et al.*, 2012]. LR-CC calculations were done using the Dalton 2015 quantum chemistry package [*Aidas et al.*, 2014]. RI-SCS-MP2 potential energy surface scans and transition state searches were done using the ORCA quantum chemistry program [*Neese*, 2012] (see supporting information section S1 for details).

Rate constants for unimolecular reactions were calculated with transition state theory (TST) without tunneling correction. The bimolecular rate constant was calculated using the calculated high pressure and experimentally determined low-pressure limit rate constant of ^{3}SO+^{3}SO association in a Troe scheme [*Troe*, 1979]. To estimate the relative abundance of the S_2O_2 isomers, we solved the master equation using the Troe rate constant for ^{3}SO+^{3}SO association and the unimolecular rate constants for reactions with barriers less than 80 kJ/mol. Reaction rates via higher-energy barriers were considered negligible, given Venus conditions at 64 km altitude.

3. Results and Discussion

Sulfur monoxide, SO, is abundant in the Venusian atmosphere. It is isovalent with O_2 and has a triplet ground state. Two ^{3}SO molecules can react in different ways leading to the S_2O_2 isomers OSSO or SOSO, which both have a *cis* and a *trans* conformers. The reaction is either barrierless or has a very small barrier (see section S2.1 in the supporting information). The relative energies of the S_2O_2 isomers and the transition states connecting these isomers are shown in Figure 1 (details are in the supporting information section S2.1).

Cis- and *trans*-OSSO are formed directly from the ^{3}SO+^{3}SO reaction and are both energetically favorable. They have nearly the same zero-point vibrational energy (ZPVE)-corrected electronic energy (*cis*-OSSO is 6.2 kJ/mol lower). The transition state, TS_3, that connects *cis*- and *trans*-OSSO is similar in energy to ^{3}SO+^{3}SO. The CCSD(T) method gives a different geometry and a higher energy for TS_3 compared to MRCI, which we suspect is due to CCSD(T) not describing the multireference character of TS_3 correctly. The CI vectors of TS_3 indicate that it is described mainly by two states, due to the π and π^* molecular orbitals along the S–S bond becoming nearly degenerate in the TS_3. The MRCI-calculated energy barrier from *trans*-OSSO to *cis*-OSSO via TS_3 is 83 kJ/mol. This translates to a slow *cis*/*trans* isomerization rate constant (10^{-7} s^{-1} at T = 245 K). The ^{3}SO+^{3}SO reaction can also lead to ^{3}OSSO formation, which has a geometry similar to that of TS_3 (see supporting information section S2.1 [*Buchachenko*, 2000]). We expect that *cis*- and *trans*-OSSO are formed in equal amounts from ^{3}SO+^{3}SO reaction since the dihedral angle of TS_3 is close to 90° in the MRCI-optimized geometry, meaning random orientation of the two ^{3}SO molecules along the dihedral angle will result in equal propensity to form *cis*-OSSO and *trans*-OSSO.

The likely formation of OSSO from ^{3}SO+^{3}SO in the Venusian atmosphere is corroborated by a laboratory experiment where *cis*-OSSO was detected by rotational spectroscopy to form from SO [*Lovas et al.*, 1974]. *Trans*-OSSO could not detected in this experiment because it has no dipole moment.

Cis-SOSO and *trans*-SOSO are close in energy to free ^{3}SO+^{3}SO, but also to the TS_4, that connects to C_1-S_2O_2. Due to these low barriers to dissociation *cis*- and *trans*-SOSO themselves are not likely to be present in significant abundance on Venus. Some C_1-S_2O_2 will be formed from *trans*-SOSO. However, the C_1-S_2O_2 isomer will dissociate upon near-UV irradiation above the cloud layer on Venus, as it has two electronic transitions in the 300–400 nm wavelength range with small oscillator strengths (10^{-4} to 10^{-3}) as well as electronic transitions in the 220–270 nm range with moderate (>0.01) oscillator strengths (see supporting information Table S10). We have solved the master equation for the system illustrated in Figure 1 containing ^{3}SO+^{3}SO, *cis*-OSSO, *trans*-OSSO, *cis*-SOSO, *trans*-SOSO, C_1-S_2O_2, TS_4, and TS_5 and conclude that formation of C_1-S_2O_2 is less significant than OSSO formation (see supporting information section S4 for details).

Table 1. Vertical Excitation Energy (Vee) and Oscillator Strengths (*f*) of the Transition to the Two Lowest Lying Electronic States in the S_2O_2 Isomers[a]

S_2O_2 isomer	Vee (nm)	*f*	Vee (nm)	*f*
cis-OSSO	443	0[b]	313	0.08891
trans-OSSO	501	0[b]	370	0.09392
Trigonal S_2O_2	313	0[b]	273	0.00134
C_1-S_2O_2	397	0.00032	305	0.00199
cis-SOSO	971	0.00001	375	0.07847
trans-SOSO	1169	0.00017	449	0.11605

[a]Calculated with LR-CC2/aug-cc-pV(T+d)Z on MRCI/cc-pV(T+d)Z optimized geometries.
[b]Symmetry forbidden transitions.

While trigonal S_2O_2 is the most stable S_2O_2 isomer, it is only formed via the C_1-S_2O_2 isomer. The MRCI barrier from C_1-S_2O_2 to trigonal S_2O_2 is 152 kJ/mol (126 kJ/mol with CCSD(T)). Thus, formation of trigonal S_2O_2 via this chemistry is not important (TST rate constant of about 10^{-20} s^{-1} at $T = 245$ K), despite previous suggestions that it was the major $(SO)_2$ isomer on Venus [*Marsden and Smith*, 1990; *Krasnopolsky*, 2012].

3.1. Formation of OSSO

We estimate the formation rate coefficient of OSSO, k_{SO+SO}, from collision theory and the *Herron and Huie* [1980] experiment (see supporting information section S4 for details). *Herron and Huie* [1980] experimentally determined a rate constant for the formation of an SO dimer (suggested here as *cis*/*trans*-OSSO) via a three-body reaction:

$$SO + SO \xrightarrow{M} (SO)_2. \quad (1)$$

The rate of OSSO formation is given by

$$\frac{d[OSSO]}{dt} = k_0[SO]^2[M] \quad (2)$$

in the low-pressure limit. The rate constant, k_0, was measured to be $k_0 = 4.4 \times 10^{-31}$ molecule^{-2} cm^6 s^{-1} at $T = 298$ K and $p = 2$ to 8 Torr of N_2 with an estimated ±50% uncertainty. Herron and Huie note that experiments at higher pressures and lower temperatures are necessary to refine the rate constant [*Herron and Huie*, 1980]. To match Venus conditions, the low-pressure limit rate constant is scaled by 3.3 to account for CO_2 being the third body [*Zhang et al.*, 2012].

The barrierless OSSO formation allows us to estimate a high-pressure limit rate constant, k_∞, with collision theory as described in the SI with calculations $k_\infty = 1.4 \times 10^{-11}$ molecule^{-1} cm^3 s^{-1} at $T = 245$ K. To model the formation rate in the Venusian atmosphere, we use a Troe scheme [*Troe*, 1979]. The rate constant k_0 from the *Herron and Huie* [1980] study (scaled by 3.3) and our estimated k_∞ are used. At 64 km altitude the rate coefficient is $k_{Troe} = 5 \times 10^{-12}$ molecule^{-1} cm^3 s^{-1} ($[M] = 3 \times 10^{18}$ molecules cm^{-3} and $T = 245$ K). Details on the calculation of the Troe rate constant is given in the supporting information section S4. Given the lack of measurements of the reaction rate for conditions relevant to Venus (64 km altitude) we have low confidence in this term. Errors as large as a factor of 3 seem possible.

3.2. Photochemical Loss of OSSO

The position and strength of the electronic transitions are necessary to estimate photolysis rates. The two lowest lying electronic transitions for each of the six identified S_2O_2 isomers are shown in Table 1. Additional higher-energy electronic transitions are given in the supporting information section S2.2.

The second electronic transition in both *cis*-OSSO ($A_1 \rightarrow B_2$) and *trans*-OSSO ($A_g \rightarrow B_u$) have significant oscillator strength in the near-UV range. At the highest level calculation, CC3/aug-cc-pV(T+d)Z, the vertical excitation energy and oscillator strength of *cis*-OSSO are 316 nm and 0.077, and for *trans*-OSSO it is 364 nm and 0.074. The vertical excitation energies and oscillator strengths were found to be insensitive to the choice of coupled-cluster method and basis set (see supporting information Tables S13 and S14). The CC3-calculated vertical excitation energies are converged (and expected accurate) to within ±2 nm and the oscillator strengths to within ±20%. While error in the calculated oscillator strength will affect the calculated

number density of OSSO, the calculated optical density of OSSO is not sensitive to these errors because, as discussed below, the total absorption rate is determined by the production rate of OSSO.

To estimate the photolysis yield of OSSO, we optimized the geometry of the second excited state of both *cis*-OSSO ($1B_2$) and *trans*-OSSO ($1B_u$). In the excited state of both isomers, the central S–S bond is elongated by around 0.4 Å. The other geometric parameters such as the S=O bond length and the internal angles were similar in the ground and excited state geometries. The energy needed for *cis*- and *trans*-OSSO to dissociate is on the order of 90 kJ/mol (see Figure 1), and thus absorption of a 320–400 nm photon will provide more than 200 kJ/mol of excess energy. Dissociation will thus result in cleavage of the S–S bond, and the photolysis of OSSO follows:

$$\mathrm{OSSO} \xrightarrow{h\nu} \mathrm{SO} + \mathrm{SO}. \tag{3}$$

With a unity quantum yield (Φ=1), the photolysis rate coefficient, J, is given by

$$J = \int_{\lambda_1}^{\lambda_2} F(\lambda) \times \sigma(\lambda)\, \mathrm{d}\lambda, \tag{4}$$

where F(λ) is the actinic flux and $\sigma(\lambda)$ is the absorption cross section. The cross section is calculated from the oscillator strength of the relevant transitions. We fitted a Lorentzian curve to the absorption cross sections of the *cis*-OSSO and *trans*-OSSO electronic transitions centered at 316 nm and 364 nm, respectively. We used a full width at half maximum (FWHM) of 0.6 eV (see supporting information Figure S5 for the altitude-dependent *J* values and Figure S7 for the computed cross sections). The FWHM was chosen based on observed FWHM of electronic absorption bands in related molecules S_2O (0.5 eV wide), S_3 (0.7 eV wide), and SO_3 (0.9 eV wide) [*Meyer et al.*, 1972; *Cordes*, 1937; *Jones*, 1950; *Cobos and Croce*, 2014; *Hintze et al.*, 2003]. The actinic flux for the Venusian atmosphere is taken from the supporting information of *Zhang et al.* [2012] We calculate the photolysis rate coefficient (lifetime) at the 64 km altitude to be 0.16 s^{-1} (6.2 s) and 0.39 s^{-1} (2.6 s) for *cis*- and *trans*-OSSO, respectively. The short lifetime of OSSO agrees with the inhomogeneous distribution and short lifetime UV dark contrasts on Venus [*Murray et al.*, 1974; *Rossow et al.*, 1980; *Molaverdikhani et al.*, 2012].

Other photochemical loss processes for OSSO were investigated. The collision frequency for OSSO, which on Venus at 64 km altitude, is about 8×10^8 s^{-1}. The number density of the Venusian atmosphere at this altitude is 3×10^{18} molecules cm^{-3} which means chemical species less abundant than approximately 3 ppb will not collide with OSSO, within its lifetime.

Most of the Venusian atmosphere consists of nonreactive CO_2 and N_2, and the only reactive species abundant enough to collide with OSSO within its lifetime is SO which has a number density of 4.1×10^{10} molecules cm^{-3} at 64 km altitude. However, the reaction, $\mathrm{OSSO} + \mathrm{SO} \rightarrow \mathrm{S_2O} + \mathrm{SO_2}$, has a rate constant of 3×10^{-14} $cm^3 s^{-1}$ [*Herron and Huie*, 1980], which implies a loss rate of 0.001 s^{-1}—approximately 100 times slower than the photolysis rate of OSSO. While this reaction will not affect the OSSO concentrations, it may provide significant S_2O concentrations and therefore be a source for other sulfur oxides on Venus. Thus, chemical reactions will be insignificant mechanisms for OSSO loss on Venus during daylight. Thermal decomposition of OSSO via collision with *M* to form two SO molecules has previously been studied and is much slower than the time scale of OSSO photolysis [*Yung and DeMore*, 1982]. We conclude that OSSO exclusively is lost via photolysis and; therefore, during daylight [OSSO] will be in photochemical steady state:

$$[\mathrm{OSSO}] = k_{\mathrm{SO+SO}} \frac{[\mathrm{SO}]^2}{J}. \tag{5}$$

The largest contributions to uncertainty in our OSSO estimate come from the uncertainty of the observationally constrained SO concentrations and in the rate coefficient. Uncertainties in our model are discussed in the supporting information section S5.

3.3. Impact of OSSO on the Venusian Atmosphere

Atmospheric models of Venus by *Krasnopolsky* [2012] assume that the SO+SO reaction produces trigonal S_2O_2, which has the photolysis product SO_2+S. *Zhang et al.* [2012], on the other hand, do not include S_2O_2 photochemistry. Here we find that S_2O_2 on Venus is in the form of *cis*-OSSO and *trans*-OSSO with SO as their only photolysis product. Given its short lifetime, OSSO can be considered an SO reservoir compound. We expect at night, for example, that all the SO will be converted to OSSO. We make two models of the OSSO mixing ratio from 58 to 112 km altitude using measurements of SO, at equatorial latitudes. For model A we use a mixing

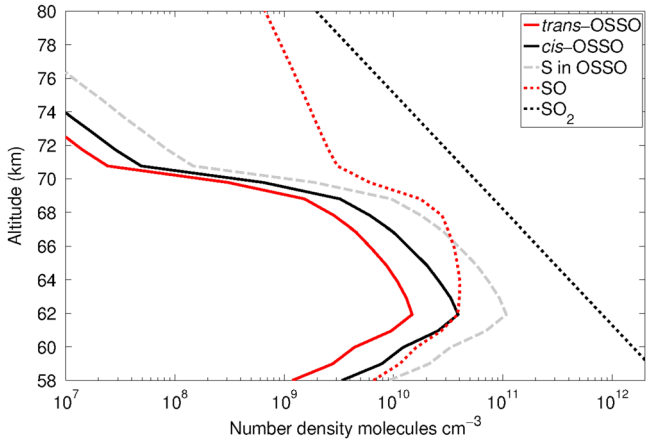

Figure 2. Altitude-dependent number densities of *cis*- and *trans*-OSSO according to our model A. The dashed gray line corresponds to 2×(*cis*-OSSO+*trans*-OSSO), representing the total amount of sulfur contained in the two OSSO isomers. SO is modeled based on a 12 ppb mixing ratio at 64 km altitude from *Na et al.* [1994] and set to 3 ppb at 70 km altitude based on *Sandor et al.* [2010]. The SO_2 line corresponds to an average mixing ratio 120 ppb at 64 km altitude and with a scale height of 3 km from *Na et al.* [1994].

ratio of 12 ppb at 64 km altitude from *Na et al.* [1994], while for model B we use a mixing ratio of 20 ppb at 64 km altitude from *Na et al.* [1990]. We note that the 12 ppb is quoted with a ±5 ppb uncertainty, and that the observation by *Na et al.* [1990] had a ±10 ppb uncertainty. The remaining fix points are identical for the two models: 3 ppb at 70 km altitude from *Sandor et al.* [2010] using their model C and 150 ppb at 96 km altitude from *Belyaev et al.* [2012]. Details on the modeled SO mixing ratios in between the fix points can be found in the supporting information section S7 where we also provide a short review of the measured SO mixing ratios.

In Figure 2, we show the concentration profile of SO used in our model A and the calculated daytime OSSO number densities. The SO_2 concentration is included for illustrative purposes in the figure [*Na et al.*, 1994, 1990]. We do not include eddy diffusion in our model, since OSSO has a lifetime of just a few seconds. At 64 km altitude the calculated [SO]/[OSSO] ratio is 1.1 for model A and 0.7 for model B, and thus, OSSO is likely a major sulfur reservoir in the Venusian mesosphere, while the partitioning between *cis*- and *trans*-OSSO was found to be 70%/30%, respectively, for both models.

The calculated rate of *cis*- and *trans*-OSSO formation together with the large absorption cross sections of these molecules implies significant opacity in the near-UV. While there remains significant uncertainties due to both the abundance of SO and the rate coefficient for the SO self-reaction, we find that this chemistry can explain a substantial fraction of the anomalous absorption noted in many observations. Recently, Haus and colleagues [*Haus et al.*, 2015, 2016] used a state-of-the-art radiative transfer model to study the UV reflectivity (albedo) of Venus. In these studies they diagnosed, as a function of wavelength, the altitude dependence of the unknown absorber required to explain the observed albedo. Because wavelength-dependent scattering by gases above the upper cloud deck contributes significantly to the UV reflectivity, Haus *et al.* described two possible vertical profiles that can produce the observed top-of-atmosphere reflectivity. In Figure 3, we reproduce the *Haus et al.* [2016] Figure 10 along with our calculation of the opacity derived from OSSO (using either model A or model B). We calculate optical depths using a Lorentzian peak shape centered at 316 nm for *cis*-OSSO and 364 nm for *trans*-OSSO with a full width at half maximum of 0.6 eV for each electronic transition. The wavelength-dependent opacity produced is quite consistent with Haus Low-Altitude Model. At wavelengths shorter than 320 nm, absorption due to the unknown agent is difficult to disentangle from absorption due to SO_2 (as shown in Figure 3) and so we do not place much weight in the disagreement at these wavelengths. The SO_2 absorption cross section was taken from literature [*Hermans et al.*, 2009]. Indeed, some of the absorption from 300 to 320 nm, previously assigned to SO_2 [*Pollack et al.*, 1979], is partially explained by *cis*-OSSO. *Molaverdikhani et al.* [2012] determined the average optical depth (OD) of the unknown absorber to be 0.21±0.04 at 365 nm, with an OD as high as 0.5 in some areas. This agrees well with both the *Haus et al.* [2015, 2016] models and our model A and model B, which is evident in Figure 3. The absorption in the 320–400 nm wavelength range is too broad to be assigned to a single gaseous absorber [*Hapke and Nelson*, 1975]. However, the calculated opacity of the absorbers, *cis*- and *trans*-OSSO, gives an absorption feature wider

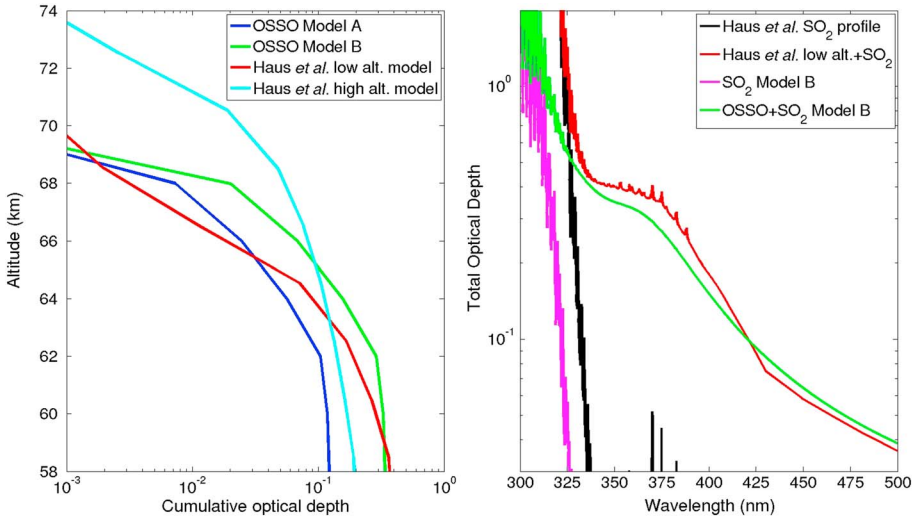

Figure 3. Optical depth of OSSO compared to the *Haus et al.* [2015, 2016] unknown UV absorber models. (left) Cumulative optical depth versus Venus altitude. Optical depth evaluated at 354 nm for OSSO and 354 nm for Haus' unknown UV absorber. (right) Wavelength versus total optical depth. The optical depth only includes SO_2 and OSSO (or the Haus retrieved UV absorber and SO_2), with all other species excluded.

than that of a single absorber. The absorption cross section for *cis*- and *trans*-OSSO used for this spectrum is shown in the supporting information section S6 and Figure S7.

4. Conclusions

We identify *cis*- and *trans*-OSSO as important sulfur reservoirs in the atmosphere of Venus. Based on observations of SO and the measured rate coefficient for its self-reaction, we estimate the formation rate of these two isomers. From calculations of the electronic transitions of these two molecules, we estimate their wavelength-dependent absorption cross sections. We find that, during daylight, the lifetime of these molecules is very short (on the order of a few seconds). We calculate the wavelength and altitude dependence of the opacity and find that it closely matches previous estimates of the optical properties of the unknown near-UV absorber. The two OSSO isomers exhibit a combined absorption over a wide spectral range, which matches that of the unknown UV absorber. The calculated mixing ratio of OSSO from our model suggests that OSSO exists in concentrations similar to the second most abundant sulfur oxide (SO) in the top cloud layer of Venus, surpassed only by SO_2.

Nevertheless, our estimate of the opacity is highly uncertain as the SO abundance is poorly constrained, and the rate coefficient for its self-reaction has been studied only once and at lower pressures compared to the pressure of upper cloud layer on Venus [*Herron and Huie*, 1980]. As the microwave spectrum of *cis*-OSSO is known [*Lovas et al.*, 1974] and the concentration of *cis*-OSSO—particularly at night—is calculated to be relatively large, observations at these wavelengths may offer the best opportunity to evaluate our hypothesis. Future modeling of the Venusian atmosphere should include OSSO and its effect on SO concentrations.

Acknowledgments
We thank Yuk L. Yung for his assistance in interpreting the contribution of OSSO to the observed near-UV opacity at Venus. We thank Veronica Vaida, Theo Kurten, Stephan P. A. Sauer, and Matthew S. Johnson for helpful discussions and Tyler Robinson for providing the digitalized files of the unknown absorber from *Haus et al.* [2015, Figure 18]. We acknowledge the financial support from the Danish Center for Scientific Computing, University of Copenhagen and the Center for Exploitation of Solar Energy founded by the University of Copenhagen. The data used are listed in the supporting information.

References

Aidas, K., et al. (2014), The Dalton quantum chemistry program system, *Wiley Interdiscip. Rev. Comput. Mol. Sci.*, *4*(3), 269–284, doi:10.1002/wcms.1172.

Arney, G., V. Meadows, D. Crisp, S. J. Schmidt, J. Bailey, and T. Robinson (2014), Spatially resolved measurements of H_2O, HCl, CO, OCS, SO_2, cloud opacity, and acid concentration in the Venus near-infrared spectral windows, *J. Geophys. Res. Planets*, *119*, 1860–1891, doi:10.1002/2014JE004662.

Barker, E. S. (1979), Detection of SO_2 in the UV Spectrum of Venus, *Geophys. Res. Lett.*, *6*, 117–120.

Barker, E. S., J. H. Woodman, M. A. Perry, B. A. Hapke, and R. Nelson (1975), Relative Spectrophotometry of Venus from 3067 to 5960 Å, *J. Atmos. Sci.*, *32*, 1205–1211.

Becke, A. D. (1993), Density-functional thermochemistry. III. The role of exact exchange, *J. Chem. Phys.*, *98*, 5648–5652.

Belyaev, D. A., F. Montmessin, J. L. Bertaux, A. Mahieux, A. A. Fedorova, O. I. Korablev, E. Marcq, Y. L. Yung, and X. Zhang (2012), Vertical profiling of SO_2 and SO above Venus' clouds by SPICAV/SOIR solar occultations, *Icarus*, *217*, 740–751.

Bernholdt, D. E., and R. J. Harrison (1996), Large-scale correlated electronic structure calculations: The RI-MP2 method on parallel computers, *Chem. Phys. Lett.*, *250*, 477–484.
Buchachenko, A. L. (2000), Recent advances in spin chemistry, *Pure Appl. Chem.*, *72*, 2243–2258.
Chai, J.-D., and M. Head-Gordon (2008), Long-range corrected hybrid density functionals with damped atom-atom dispersion corrections, *Phys. Chem. Chem. Phys.*, *10*, 6615–6620.
Chen, W. K., J. Q. Li, Y. F. Zhang, K. N. Ding, and Y. Li (2004), DFT study on the stabilities of disulfur dioxide isomers, *Chin. J. Struct. Chem.*, *23*, 469–473.
Christiansen, O., H. Koch, and P. Jørgensen (1995), The second-order approximate coupled cluster singles and doubles model CC2, *Chem. Phys. Lett.*, *243*, 409–418.
Cobos, C. J., and A. E. Croce (2014), Theoretical study of the electronic spectrum of disulfur monoxide, *Z. Naturforsch., A: Phys. Sci.*, *69*, 215–219.
Coffeen, D. L. (1971), Venus Cloud Contrasts, *Int. Astron. Congr.*, SAO/NASA Astrophysics Data System. [Available at www.adsabs.harvard.edu.]
Cordes, H. (1937), Über ein neues Absorptionsspektrum des zweiatomigan Schwefels, *Z. Phys.*, *105*, 251–264.
Dunne, J. A. (1974), Mariner 10 Venus encounter, *Am. Assoc. Adv. Sci.*, *183*, 1289–1291.
Dunning, T. H., Jr., K. A. Peterson, and A. K. Wilson (2001), Gaussian basis sets for use in correlated molecular calculations. X. The atoms aluminum through argon revisited, *J. Chem. Phys.*, *114*, 9244–9253.
Encrenaz, T., T. K. Greathouse, H. Roe, M. Richter, J. Lacy, B. Bezard, T. Fouchet, and T. Widemann (2012), HDO and SO_2 thermal mapping on Venus: Evidence for strong SO_2 variability, *Astron. Astrophys.*, *543*, A153.
Encrenaz, T., T. K. Greathouse, M. J. Richter, J. Lacy, T. W. B. Bezard, T. Fouchet, C. deWitt, and S. K. Atreya (2013), HDO and SO_2 thermal mapping on Venus: II. The SO_2 spatial distribution above and within the clouds, *Astron. Astrophys.*, *559*, A65.
Esposito, L. W. (1984), Sulfur dioxide: Episodic injection shows evidence for active Venus volcanism, *Science*, *223*, 1072–1074.
Esposito, L. W., and L. D. Travis (1982), Polarization studies of the Venus UV contrasts: Cloud height and haze variability, *Icarus*, *51*, 374–390.
Esposito, L. W., J. R. Winick, and A. Ian Stewart (1979), Sulfur dioxide in the Venus atmosphere: Distribution and implications, *Geophys. Res. Lett.*, *6*, 601–604.
Esposito, L. W., M. Copley, R. Eckert, L. Gates, A. I. F. Stewart, and H. Worden (1988), Sulfur dioxide at the Venus cloud tops, 1978–1986, *J. Geophys. Res.*, *93*, 5267–5276.
Feyereisen, M., G. Fitzgerald, and A. Komornicki (1993), Use of approximate integrals in ab initio theory. An application in MP2 energy calculations, *Chem. Phys. Lett.*, *208*, 359–363.
Frisch, M. J., et al. (2009), *Gaussian 09, Revision B.01*, Gaussian Inc., Wallingford CT.
Goodarzi, M., M. Vahedpour, and F. Nazari (2010), Theoretical study on the atmospheric formation of *cis* and *trans*-OSSO complexes, *Chem. Phys. Lett.*, *494*, 315–322.
Grimme, S. (2003), Improved second-order Møller-Plesset perturbation theory by separate scaling of parallel- and antiparallel-spin pair correlation energies, *J. Chem. Phys.*, *118*, 9095–9102.
Hapke, B., and R. Nelson (1975), Evidence for an elemental sulfur component of the clouds from Venus spectrophotometry, *J. Atmos. Sci.*, *32*, 1212–1218.
Hartley, K. K., A. R. Wolff, and L. D. Travis (1989), Croconic acid: An absorber in the Venus clouds?, *Icarus*, *77*, 382–390.
Haus, R., D. Kappel, and G. Arnold (2015), Radiative heating and cooling in the middle and lower atmosphere of Venus and responses to atmospheric and spectroscopic parameter variations, *Planet. Space Sci.*, *117*, 262–294.
Haus, R., D. Kappel, S. Tellmann, G. Arnold, G. Piccioni, P. Drossart, and B. Husler (2016), Radiative energy balance of Venus based on improved models of the middle and lower atmosphere, *Icarus*, *272*, 178–205.
Hermans, C., A. C. Vandaele, and S. Fally (2009), Fourier transform measurements of SO_2 absorption cross sections: I. Temperature dependence in the 24000–29000 cm^{-1} (345–420 nm) region, *J. Quant. Spectrosc. Radiat. Transfer*, *110*, 756–765.
Herron, J. T., and R. E. Huie (1980), Rate constants at 298 K for the reactions SO+SO+M → $(SO)_2$+M and SO+$(SO)_2$ → SO_2+S_2O, *Chem. Phys. Lett.*, *76*, 322–324.
Hintze, P. E., H. G. Kjaergaard, V. Vaida, and J. B. Burkholder (2003), Vibrational and electronic spectroscopy of sulfuric acid vapor, *J. Phys. Chem. A*, *107*, 1112–1118.
Jessup, K. L., et al. (2015), Coordinated Hubble Space Telescope and Venus Express Observations of Venus' upper cloud deck, *Icarus*, *258*, 309–336.
Jones, A. V. (1950), Infra-red and ultraviolet spectra of sulphur monoxide, *J. Chem. Phys.*, *18*, 1263–1268.
Jurečka, P., J. Šponer, J. Černý, and P. Hobza (2006), Benchmark database of accurate (MP2 and CCSD(T) complete basis set limit) interaction energies of small model complexes, DNA base pairs, and amino acid pairs, *Phys. Chem. Chem. Phys.*, *8*, 1985–1993.
Kánnar, D., and P. Szalay (2014), Benchmarking coupled cluster methods on valence singlet excited states, *J. Chem. Theory Comput*, *10*, 3757–3765.
Koch, H., O. Christiansen, P. Jørgensen, A. M. Sanchez de Merás, and T. Helgaker (1997), The CC3 model: An iterative coupled cluster approach including connected triples, *J. Chem. Phys.*, *106*, 1808–1818.
Krasnopolsky, V. A. (2006), Chemical composition of Venus atmosphere and clouds: Some unsolved problems, *Planet. Space Sci.*, *54*, 13–14.
Krasnopolsky, V. A. (2008), High-resolution spectroscopy of Venus: Detection of OCS, upper limit to H_2S, and latitudinal variations of CO and HF in the upper cloud layer, *Icarus*, *197*, 377–385.
Krasnopolsky, V. A. (2012), A photochemical model for the Venus atmosphere at 47–112 km, *Icarus*, *218*, 230–246.
Lane, J. R., and H. G. Kjaergaard (2008), Calculated electronic transitions in sulfuric acid and implications for its photodissociation in the atmosphere, *J. Phys. Chem. A*, *112*, 4958–4964.
Lee, C., W. Yang, and R. G. Parr (1988), Development of the Colle-Salvetti correlation-energy formula into a functional of the electron density, *Phys. Rev. B*, *37*, 785–789.
Lee, T. J., and P. R. Taylor (1989), A diagnostic for determining the quality of single-reference electron correlation methods, *Int. J. Quantum Chem.*, *23*, 199–207.
Lee, Y. J., T. Imamura, S. E. Schröder, and E. Marcq (2015), Long-term variations of the UV contrast on Venus observed by the Venus monitoring camera on board Venus Express, *Icarus*, *253*, 1–15.
Lovas, F. J., E. Tiemann, and D. R. Johnson (1974), Spectroscopic studies of the SO_2 discharge system. II. Microwave spectrum of the SO dimer, *J. Chem. Phys.*, *60*, 5005–5010.

Marcq, E., B. Bezard, T. Encrenaz, and M. Birlan (2005), Latitudinal variations of CO and OCS in the lower atmosphere of Venus from near-infrared nightside spectro-imaging, *Icarus*, *179*, 375–386.
Marcq, E., T. Encrenaz, B. Bezard, and M. Birlan (2006), Remote sensing of Venus' lower atmosphere ground-based IR spectroscopy: Latitudinal and vertical distribution of minor species, *Planet. Space Sci.*, *54*, 1360–1370.
Marcq, E., B. Bezard, P. Drossart, G. Piccioni, J. M. Reess, and F. Henry (2008), A latitudinal survey of CO, OCS, H_2O and SO_2 in the lower atmosphere of Venus: Spectroscopic studies using VIRTIS-H, *J. Geophys. Res.*, *113*, E00B07, doi:10.1029/2008JE003074.
Marcq, E., D. Belyaev, F. Montmessin, A. Fedorova, J.-L. Bertaux, A. C. Vandaele, and E. Neefs (2011), An investigation of the SO_2 content of the Venusian mesosphere using SPICAV-UV in nadir mode, *Icarus*, *211*, 58–69.
Marcq, E., J.-L. Bertaux, F. Montmessin, and D. Belyaev (2013), Variations of sulphur dioxide at the cloud top of Venus's dynamic atmosphere, *Nat. Geosci.*, *6*, 25–28.
Markiewicz, W. J., E. Petrova, O. Shalygina, M. Almeida, D. V. Titov, S. S. Limaye, N. Ignatiev, T. Roatsch, and K. D. Matz (2014), Glory on Venus cloud tops and the unknown UV absorber, *Icarus*, *234*, 200–203.
Marsden, C. J., and B. J. Smith (1990), An ab initio study of many isomers of S_2O_2. A combined theoretical and experimental analysis of the harmonic force field and molecular structure of cis-planar OSSO, *Chem. Phys.*, *141*, 335–353.
Meyer, B., T. Stroyer-Hansen, and T. V. Oommen (1972), The visible spectrum of S_3 and S_4, *J. Mol. Spectrosc.*, *42*, 335–343.
Miliordos, E., and S. S. Xantheas (2014), On the bonding nature of ozone (O_3) and its sulfur-substituted analogues SO_2, OS_2, and S_3: Correlation between their biradical character and molecular properties, *Int. J. Chem. Kinet.*, *136*, 2808–2817.
Molaverdikhani, K., K. McGouldrick, and L. W. Esposito (2012), The abundance and vertical distribution of the unknown ultraviolet absorber in the Venusian atmosphere from analysis of Venus monitoring camera images, *Icarus*, *217*, 648–660.
Murakami, Y., S. Onishi, T. Kobayashi, N. Fujii, N. Isshiki, K. Tsuchiya, A. Tezaki, and H. Matsui (2003), High temperature reaction of $S+SO_2 \rightarrow SO+SO$: Implication of S_2O_2 intermediate complex formation, *J. Phys. Chem. A.*, *107*, 10,996–11,000.
Murray, B. C., et al. (1974), Venus—Atmospheric motion and structure from Mariner 10 pictures, *Science*, *183*, 1307–1315.
Na, C. Y., and L. W. Esposito (1997), Is disulfur monoxide a second absorber on Venus?, *Icarus*, *125*, 364–368.
Na, C. Y., L. W. Esposito, and T. E. Skinner (1990), International ultraviolet explorer observation of Venus SO_2 and SO, *J. Geophys. Res.*, *95*, 7485–7491.
Na, C. Y., L. W. Esposito, W. E. McClintock, and C. A. Barth (1994), Sulfur dioxide in the atmosphere of Venus II. Modeling results, *Icarus*, *112*, 389–395.
Neese, F. (2012), The ORCA program system, *Wiley Interdiscip. Rev. Comput. Mol. Sci.*, *2*, 73–78.
Palmer, K. F., and D. Williams (1975), Optical constants of sulfuric acid; Application to the clouds of Venus?, *Appl. Opt.*, *14*, 208–219.
Parkinson, C. D., P. Gao, L. Esposito, Y. Yung, S. Bougher, and M. Hirtzig (2015), Photochemical control of the distribution of Venusian water, *Planet. Space Sci.*, *113–114*, 226–236.
Pollack, J. B., B. Ragent, R. Boese, M. G. Tomasko, J. Blamont, R. G. Knollenberg, L. W. Esposito, A. I. Stewart, and L. Travis (1979), Nature of the ultraviolet absorber in the Venus clouds: Inferences based on pioneer Venus data, *Science*, *205*, 76–79.
Pollack, J. B., O. B. Toon, R. C. Whitten, R. Boese, B. Ragent, M. Tomasko, L. Esposito, L. Travis, and D. Wiedman (1980), Distribution and source of the UV absorption in Venus' atmosphere, *J. Geophys. Res.*, *85*, 8141–8150.
Purvis, G. D., and R. J. Bartlett (1982), *A full coupled-cluster singles and doubles model: The inclusion of disconnected triples*, *76*, 1910–1918.
Raghavachari, K., G. W. Trucks, J. A. Pople, and M. Head-Gordon (1989), A fifth-order perturbation comparison of electron correlation theories, *Chem. Phys. Lett.*, *157*, 479–483.
Ramírez-Solís, A., F. Jolibois, and L. Maron (2011), Born-Oppenheimer DFT molecular dynamics studies of S_2O_2 non-harmonic effects on the lowest energy isomers, *Chem. Phys. Lett.*, *510*, 21–26.
Ross, F. E (1928), Photographs of Venus, *Astrophys. J.*, *68*, 57–92.
Rossi, E., G. L. Bendazzoli, S. Evangelisti, and D. Maynau (1999), A full-configuration benchmark for the N_2 molecule, *Chem. Phys. Lett.*, *310*, 530–536.
Rossow, W. B., A. D. Del Genio, S. S. Limaye, L. D. Travis, and P. H. Stone (1980), Cloud morphology and motions from pioneer Venus images, *J. Geophys. Res.*, *85*, 8107–8128.
Rossow, W. B., A. D. Del Genio, and T. Eichler (1990), Cloud-tracked winds from pioneer Venus OCPP images, *J. Atmos. Sci.*, *47*, 2053–2084.
Sandor, B. J., R. T. Clancy, G. Moriarty-Schieven, and F. P. Mills (2010), Sulfur chemistry in the Venus mesosphere from SO_2 and SO microwave spectra, *Icarus*, *208*, 740–751.
Seiff, A., et al. (1985), Models of the structure of the atmosphere of Venus from the surface to 100 kilometers altitude, *Adv. Space Res.*, *5*, 3–58.
Shamasundar, K. R., G. Knizia, and H.-J. Werner (2011), A new internally contracted multi-reference configuration interaction method, *J. Chem. Phys.*, *135*, 054101.
Sherrill, C. D., and H. F. Schaefer (1999), The configuration interaction method: Advances in highly correlated approaches, *Adv. Quantum Chem.*, *34*, 143–269.
Titov, D. T., F. W. Taylor, H. Svedhem, N. I. Ignatiev, W. J. Markiewicz, G. Piccioni, and P. Drossart (2008), Atmospheric structure and dynamics as the cause of ultraviolet markings in the clouds of Venus, *Nat. Lett.*, *456*, 620–623.
Titov, D. V., et al. (2006), Venus Express: Scientific goals, instrumentation, and scenario of the mission, *Cosmic Res.*, *44*, 334–348.
Toon, O. B., R. P. Turco, and J. B. Pollack (1982), The ultraviolet absorber on Venus: Amorphous sulfur, *Icarus*, *51*, 358–373.
Travis, L. D. (1975), On the origin of ultraviolet contrasts on Venus, *J. Atmos. Sci.*, *32*, 1190–1200.
Troe, J. (1979), Predictive possibilities of unimolecular rate theory, *J. Phys. Chem.*, *83*, 114–126.
Vandaele, A. C., C. Hermans, P. C. Simon, and M. V. Roozendael (1996), Fourier transform measurement of NO_2 absorption cross-section in the visible range at room temperature, *J. Atmos. Chem.*, *25*, 289–305.
Werner, H.-J., and P. J. Knowles (1988), An efficient internally contracted multiconfiguration–reference configuration interaction method, *J. Chem. Phys.*, *89*, 5803–5814.
Werner, H. J. et al. (2012), Molpro quantum chemistry package. [Available at http://www.molpro.net/, Accessed date 9 Jan 2014.]
Yung, Y. L., and W. B. DeMore (1982), Photochemistry of the stratosphere of Venus: Implication for atmospheric evolution, *Icarus*, *51*, 199–247.
Yung, Y. L., M. C. Liang, X. Jiang, R. L. Shia, C. Lee, B. Bezard, and E. Marcq (2009), Evidence for carbonyl sulfide (OCS) conversion to CO in the lower atmosphere of Venus, *J. Geophys. Res.*, *114*, E00B34, doi:10.1029/2008JE003094.
Zasova, L. V., V. A. Krasnopolsky, and V. I. Moroz (1981), Vertical distribution of SO_2 in upper cloud layer of Venus and origin of U.V.-absorption, *Adv. Space Res.*, *1*, 13–16.

Zhang, X., M.-C. Liang, F. Montemssin, J.-L. Bertaux, C. Parkinson, and Y. L. Yung (2010), Photolysis of sulphuric acid as the source of sulphur oxides in the mesosphere of Venus, *Nat. Geosci.*, *3*, 834–837.

Zhang, X., M.-C. Liang, F. P. Mills, D. A. Belyaev, and Y. L. Yung (2012), Sulfur chemistry in the middle atmosphere of Venus, *Icarus*, *217*, 714–739.

Zhao, Y., and D. G. Truhlar (2008), The M06 suite of density functionals for main group thermochemistry, thermochemical kinetics, noncovalent interactions, excited states, and transition elements: Two new functionals and systematic testing of four M06-class functionals and 12 other functionals, *Theor. Chem. Acc.*, *120*, 215–241.